Peertechz

International Journal of
Nanomaterials, Nanotechnology and Nanomedicine

ISSN: 2455-3492 Journal DOI: https://dx.doi.org/10.17352/ijnnn

Research Article

Fabrication and Characterization of Cosmetic-grade TiO_2@SiO_2 for UV-shielding Ingredient

Wenrong Xiang, Rui Liu, Jiesong Liu, Chengxue Du and Li Li*

College of Chemistry and Chemical Engineering, Chongqing University of Technology, Chongqing 400054, China

Submitted : 21 January, 2026
Accepted : 29 January, 2026
Published : 30 January, 2026

***Corresponding author:** Li Li, College of Chemistry and Chemical Engineering, Chongqing University of Technology, Chongqing 400054, China,
E-mail: chenlili@cqut.edu.cn

Keywords: TiO_2@SiO_2; Core-shell structure; UV-shielding; SPF; Sunscreen; Oil absorption

https://www.chemisgroup.us

Check for updates

Abstract

Nanoscale TiO_2 generates reactive oxygen species (ROS) under ultraviolet (UV) radiation, causing damage to biological systems and polymers. To mitigate associated health risks in cosmetic applications, TiO_2 core-shell materials were synthesized. This study describes the fabrication of TiO_2@SiO_2 core-shell materials utilizing a chemical deposition technique with nanoscale TiO_2 and sodium silicate (Na_2SiO_2) as precursors. The outcomes demonstrated that the morphology, configuration, and light-interacting properties of the surface-coated SiO_2 shell are governed by the solution's pH value. Under alkaline conditions, it can obtain a uniform and dense continuous SiO_2 shell layer, which not only improves the whiteness and brightness of TiO_2 but also reduces oil absorption. The TiO_2@SiO_2-10 sample exhibited a sun protection factor (SPF) of 41 ± 2, suggesting potential for cosmetic-grade UV filters. Process simplicity further supports practical applicability.

Introduction

The depletion of the ozone layer has led to increased ultraviolet (UV) radiation exposure, causing significant adverse effects on human skin, polymeric materials, and surface coatings [1,2]. The use of ultraviolet protective agents can effectively prevent skin sunburn, aging of polymer and coating, such as surface weathering, yellowing, brittleness, and photodegradation caused by UV radiation [3-5]. The UV-shielding agents are broadly categorized into organic absorbers and inorganic blockers. In contrast to organic counterparts, inorganic UV blockers offer distinct advantages, including extended spectral coverage, superior photostability, and enhanced biocompatibility [6,7]. Hawaii recently prohibited the sale of over-the-counter sunscreens containing certain organic ultraviolet absorbers to safeguard its marine environment. This action highlights the urgent need for research into safe and cost-effective inorganic alternatives [8]. Specifically, rutile TiO_2 nanoparticles, functioning as inorganic ultraviolet screening agents, have been extensively applied in sun-protection products, polymeric matrices, and automotive finishing layers [9,10]. However, despite its commercial utilization, nano TiO_2 exhibits significant photocatalytic activity and a tendency to aggregate. These characteristics pose potential risks, as photocatalytic behavior can generate reactive oxygen species harmful to organic molecules, potentially causing damage to skin and accelerating the degradation of plastic products, while aggregation reduces dispersion stability and effectiveness [11,12].

Much of the debate about the nano-TiO_2 reflects the fact that the photostability of these particles depends on the surface coating as well as crystal structure. So, the rutile TiO_2 with less photocatalytic activity is preferred over the highly photocatalytic activity anatase TiO_2, and inert oxide layers such as SiO_2 and Al_2O_3 are coated on its surface [13]. Substantial research efforts have focused on developing facile and efficient strategies for fabricating SiO_2 coatings on TiO_2 particles. The coating techniques encompass

Citation: Xiang W, Liu R, Liu J, Du C, Li L. Fabrication and Characterization of Cosmetic-grade TiO_2@SiO_2 for UV-shielding Ingredient. Int J Nanomater Nanotechnol Nanomed. 2026;12(1):0-11-017. Available from: https://dx.doi.org/10.17352/2455-3492.000074

the Stöber approach [9,14], microwave (MV) irradiation [15,16], sol–gel synthesis [17,18], and flame spray pyrolytic processing [19,20]. The hydrothermal synthesis of rutile TiO_2 hierarchical microspheres possessing calliandra-like morphology was reported by Wang, et al. [21], with titanium(IV) isopropoxide serving as the precursor. The material exhibited high UV-shielding efficiency, effectively blocking ultraviolet radiation below 400 nm. Previous studies have found that the porosity and thickness of the SiO_2 shell play an important role in suppressing the photocatalytic activity of TiO_2. In order to obtain a dense SiO_2 coating layer, people usually use the solvothermal method for coating [22,23]. Cheepborisutikul, et al. [24] employed a sol-gel process involving tetraethyl orthosilicate hydrolysis and condensation to deposit homogeneous silica coatings on TiO_2 particles. Subsequent calcination at 1000 °C densified the SiO_2 layer, achieving a significantly reduced decomposition rate constant (0.01 h^{-1}) through triple-coating cycles that produced ~7 nm-thick dense shells. Chen, et al. [25] fabricated TiO_2@SiO_2 core-shell particles through in situ hydrolysis-condensation of tetraethyl orthosilicate on TiO_2 surfaces. The continuous, dense SiO_2 coating not only effectively suppressed the photocatalytic activity of TiO_2 but also enhanced dispersion stability and UV-shielding efficacy. Despite significant advancements over the past ten years in synthesizing TiO_2-coated SiO_2 and improving its UV resistance, challenges remain that hinder its widespread industrial utilization. Conventional methods employing ethyl orthosilicate (TEOS) as a precursor for SiO_2 coating require significant quantities of organic solvents, raising environmental concerns. Furthermore, while thicker SiO_2 shells effectively suppress the undesirable photocatalytic activity of TiO_2, they also unintentionally compromise its UV shielding efficacy. Therefore, achieving a dense SiO_2 shell via a simple and cost-effective encapsulation method that simultaneously provides effective photocatalytic suppression and high UV shielding performance remains a significant challenge.

In this study, the shell thickness and microprosity of SiO_2 coated or deposited on the TiO_2 particle surfaces were controlled with the intention of UV absorption and skin sensation of the composite. We employed sodium silicate as a precursor to deposit SiO_2 coatings onto rutile TiO_2 surfaces via acid-base neutralization. Precise control over SiO_2 morphology and pore architecture was achieved by modulating the reaction pH. In the TiO_2@SiO_2 composite system, the densely packed SiO_2 coating layer limits the ultraviolet light absorption of TiO_2 nanoparticles, which markedly reduces the formation of reactive species such as superoxide and hydroxyl radicals. Consequently, this suppression leads to a significant decrease in the photocatalytic degradation performance of the material.

Experimental section

Materials

Sodium silicate ($Na_2SiO_3 \cdot 9H_2O$) was procured from Sinopharm Chemical Reagent Co., Ltd. (Shanghai, China). Chengdu Ke Long Reagent Co., Ltd. (Chengdu, China) supplied sulfuric acid (H_2SO_4), oxalic acid, and sodium hydroxide (NaOH). The Pangang Group Research Institute Co., Ltd. provided rutile-phase nano-TiO_2. All reagents were utilized as received without further purification. Double-distilled water was employed throughout the experiments.

Synthesis

Fifty grams of TiO_2 nanoparticles were dispersed in 100 mL of deionized water and subjected to ultrasonic treatment for 20 minutes to achieve a uniform suspension. The prepared TiO_2 dispersion was then transferred into a flask and continuously stirred at 300 rpm within a water bath set to 90 °C. Concurrently, solutions of 0.15 mol·L^{-1} sodium silicate and 10% sulfuric acid were introduced into the suspension via two precision-controlled pumps over 3 hours, maintaining a constant flow rate for the sodium silicate solution. The mass ratio of SiO_2 to TiO_2 was fixed at 1:10 throughout the coating process. The pH was actively maintained between 9.5 and 10 by adjusting the addition rate of the sulfuric acid solution. After completing the reagent addition, the suspension was aged under stirring at 90 °C for 1 hour. Thereafter, the pH was fine-tuned to approximately 7.5–7.8 by incremental addition of either 10% sulfuric acid or 10% sodium hydroxide solution, followed by a further aging step lasting 2 hours. The resulting material was collected by filtration, rinsed thoroughly with deionized water, and dried at 120 °C for 12 hours. Samples prepared at different pH levels during the sodium silicate addition were designated TiO_2@SiO_2-X, where X corresponds to the pH value maintained during coating.

Characterization

The crystal structures of the samples were examined using X-ray diffraction (XRD, EMPYREAN, Panalytical) with Cu Kα radiation as the X-ray source. Morphological features and elemental compositions were investigated by transmission electron microscopy (TEM) coupled with energy dispersive spectroscopy (EDS) (Talos F200S, Thermo Fisher). Specific surface areas were determined via nitrogen adsorption–desorption isotherms measured on a 3S-2000PSI analyzer (BeiShiDe), with the Brunauer–Emmett–Teller (BET) method employed to calculate the SBET values. Chemical states and elemental compositions were further characterized by X-ray photoelectron spectroscopy (XPS, ESCALAB 250Xi, Thermo Fisher) using an Al Kα radiation source. Ultraviolet–visible (UV-vis)

Citation: Xiang W, Liu R, Liu J, Du C, Li L. Fabrication and Characterization of Cosmetic-grade TiO_2@SiO_2 for UV-shielding Ingredient. Int J Nanomater Nanotechnol Nanomed. 2026;12(1):0-11-017. Available from: https://dx.doi.org/10.17352/2455-3492.000074

diffuse reflectance spectra were recorded with a UV-2700i spectrophotometer (SHIMADZU), employing $BaSO_4$ as the reflectance standard. Whiteness values were quantified based on the CIE-L*ab** 1976 color space using a Datacolor 800V spectrophotometer. Oil absorption measurements were conducted following a spatula rub-out method analogous to ASTM Standard D281-95.

Results and discussion

Figure 1 shows the comparison of the transmission electron microscope (TEM) image of uncoated titanium dioxide nanoparticles and silicon dioxide-coated titanium dioxide samples prepared under different pH conditions. As shown in Figure 1(a), the uncoated titanium dioxide nanoparticles are elliptical, with a short axis size of about 15-20 nm and a long axis range of 45-60 nm. It was observed that the morphology of the silicon dioxide coating layer strongly depends on the pH of the reaction medium. Under alkaline conditions (pH ≥ 9), titanium dioxide nanoparticles are evenly covered by a continuous silicon dioxide shell. As shown in Figures 1(e) and 1(f), when the pH value rises to about 10, the silicon dioxide layer becomes denser and more uniform, with an average thickness of nearly 3 nanometers. Under the condition of slightly lower pH (about 9), a thicker silicon dioxide shell (about 5 nanometers) was formed, but the porosity of the coating layer increased. In contrast, as shown in Figures 1(g) and 1(h), the near-neutral pH conditions cause the surface of titanium dioxide to form a discontinuous island-like silica morphology, and the transverse size of these silicon dioxide islands is about 10-13 nanometers. Interestingly, when the pH value is further reduced to 4, the size of the silicon dioxide area decreases (5-8 nanometers), and the coating continuity is enhanced. Based on these observations, it can be concluded that increasing the pH of the reaction solution is conducive to the formation of a dense, continuous, and uniform silicon dioxide shell on the surface of titanium dioxide nanoparticles.

In order to further verify the existence of the silicon dioxide coating layer and analyze it quantitatively, the energy dispersion spectrum (EDS) analysis of TiO_2@SiO_2 samples was carried out (Figure S1 and Table S1). The results clearly confirm the presence of titanium and silicon elements in all samples, which provides direct chemical evidence in support of the morphological observation of TEM. Figure 2 (b-d) shows the surface distribution images corresponding to the elements of titanium, oxygen, and silicon, respectively. The analysis of elemental distribution and relative strength shows that titanium and oxygen are the main elements, which is in line with the expectations of titanium dioxide core materials; the silicon element content is small but clearly measurable, which is consistent with the structural characteristics of the thin shell. Most

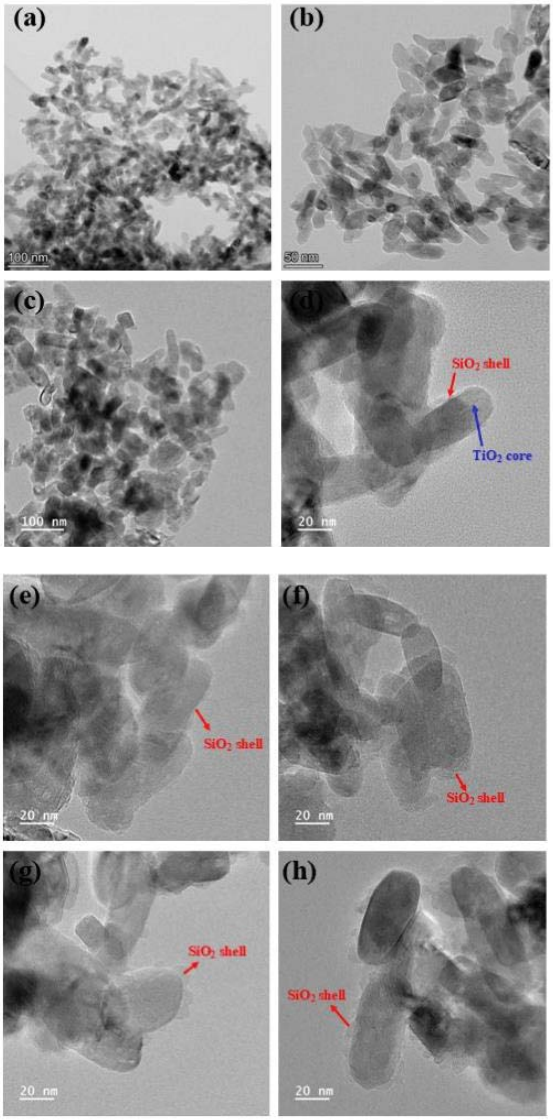

Figure 1: TEM images of (a,b) the nanoTiO_2 and (c,d) TiO_2@SiO_2 -10, (e) TiO_2@SiO_2-9, (f) TiO_2@SiO_2 -7, (g) TiO_2@SiO_2 -5, (h) TiO_2@SiO_2 -4.

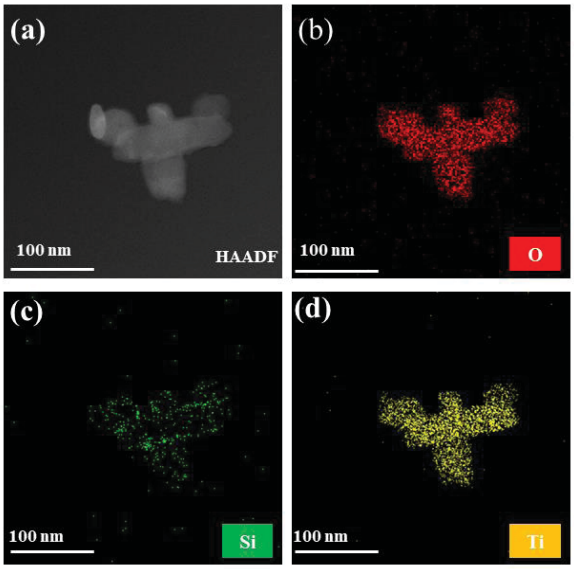

Figure 2: EDS mapping of the TiO_2@SiO_2-10 sample.

Citation: Xiang W, Liu R, Liu J, Du C, Li L. Fabrication and Characterization of Cosmetic-grade TiO_2@SiO_2 for UV-shielding Ingredient. Int J Nanomater Nanotechnol Nanomed. 2026;12(1):0-11-017. Available from: https://dx.doi.org/10.17352/2455-3492.000074

importantly, as shown in Figure 2, silicon elements are observed uniformly dispersed on the entire surface of titanium dioxide nanoparticles. This uniform distribution provides key evidence for real shell formation (not a simple physical mixture of titanium dioxide and silicon dioxide particles), confirming that the synthesis method successfully prepared a uniform core-shell structure in the whole sample. The complete surface coverage shown by the silicon element surface distribution map is crucial to ensure consistent ultraviolet protection and surface passivation performance in actual sun protection applications.

XRD analysis was performed to verify the crystalline phases and determine whether the SiO_2 coating affects the TiO_2 core structure. As shown in Figure 3, the diffraction spectrum of uncoated titanium dioxide and all silicon-coated titanium dioxide samples corresponds to rutile-type titanium dioxide, showing sharp and strong diffraction peaks unique to highly crystalline materials. The diffraction peaks at 2θ angles 27.4°, 36.2°, 41.3°, 44.1°, 54.3°, 56.6°, 62.7°, and 68.1° belong to (110), (101), (111), (210), (211) of rutile titanium dioxide, respectively. (220), (002) and (301) crystal surface (JCPDS No. 21-1276) [26,27]. These well-preserved rutile characteristic peaks do not shift the peak position, and there is no additional heterophase, which proves that silicon dioxide coating does not change the crystal structure of titanium dioxide, which is crucial to maintaining the light stability and ultraviolet barrier performance of the material. It is worth noting that amorphous silica characteristic peaks, which usually appear around 22.3°, were not detected in silicon dioxide-covered titanium dioxide samples. The reason for the absence of this peak is that: first, the silicon dioxide content is low, which is lower than the detection limit of XRD for amorphous materials; second, it forms an ultra-thin homogeneous amorphous layer instead of crystalline silicon dioxide particles [14,28].

XPS was employed to investigate the surface composition and electronic environment of the nanoparticles. The full survey spectra are presented in Figure 4(a), where TiO_2@SiO_2-10 exhibits two prominent peaks at 152.06 eV and 103.53 eV, corresponding to Si 2s and Si 2p orbitals, respectively, providing direct evidence of silicon incorporation. As shown in Figure 4(b), the Ti $2p_3/_2$ and Ti $2p_1/_2$ peaks of pristine TiO_2 appear at 458.35 eV and 464.05 eV. Upon SiO_2 coating, these peaks in TiO_2@SiO_2-10 shift to higher binding energies of 458.67 eV and 464.40 eV, respectively [28,29]. This positive shift is particularly significant as it demonstrates strong electronic interaction between the coating and core materials. The O 1s spectrum of bare TiO_2 displays two peaks at 529.63 eV and 530.37 eV, assigned to Ti–O bonds and surface hydroxyl groups. After SiO_2 deposition, the O 1s spectrum of TiO_2@SiO_2-10 reveals three distinct peaks at 529.95 eV, 531.23 eV, and

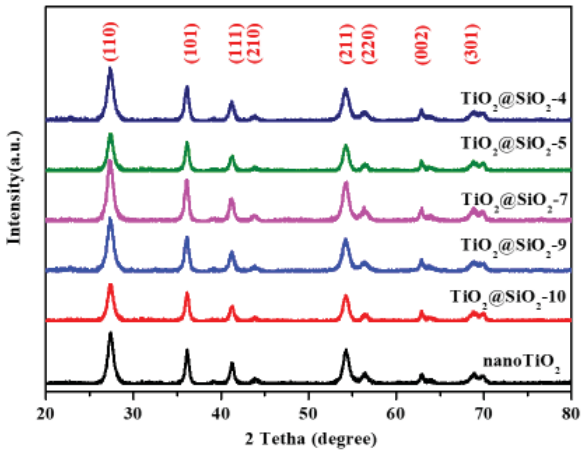

Figure 3: XRD patterns of nanoTiO_2 and TiO_2@SiO_2 samples.

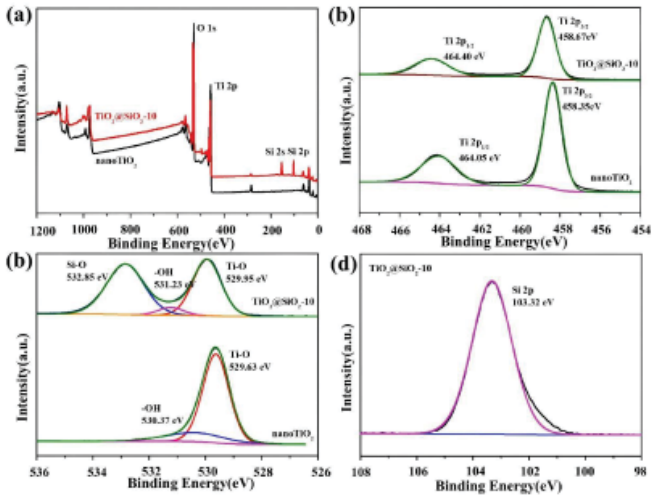

Figure 4: XPS of nanoTiO_2 and TiO_2@SiO_2-10 sample. (a) full range XPS spectra, (b) Ti 2p, (c) O 1s, (d) Si 2p spectra.

532.85 eV, corresponding to Ti–O–Ti, Ti–O–Si, and Si–O–Si bonds, respectively [30,31]. Critically, the emergence of the Ti–O–Si peak at 531.23 eV serves as definitive evidence of chemical bonding at the core-shell interface rather than simple physical deposition. The systematic shift toward higher binding energies is attributed to silicon's higher electronegativity, which withdraws electron density from titanium atoms, thereby reducing the shielding effect [14]. Additional XPS spectra of other samples are provided in Figures S2–S4. These findings conclusively demonstrate successful SiO_2 coating with strong interfacial Ti–O–Si bonding on TiO_2 nanoparticle surfaces.

FT-IR spectroscopy was employed to identify chemical functional groups and verify interfacial bonding in the TiO_2@SiO_2 composites. The FTIR spectra of nano-TiO_2 and TiO_2@SiO_2-10 are presented in Figure 5. Broad absorption bands at 3438 cm^{-1} and 1619 cm^{-1} correspond to stretching and bending vibrations of hydroxyl groups (–OH) from adsorbed water [14]. Critically, the SiO_2-coated spectrum exhibits distinct new bands at 1226 cm^{-1}, 1077 cm^{-1}, and

Citation: Xiang W, Liu R, Liu J, Du C, Li L. Fabrication and Characterization of Cosmetic-grade TiO_2@SiO_2 for UV-shielding Ingredient. Int J Nanomater Nanotechnol Nanomed. 2026;12(1):0-11-017. Available from: https://dx.doi.org/10.17352/2455-3492.000074

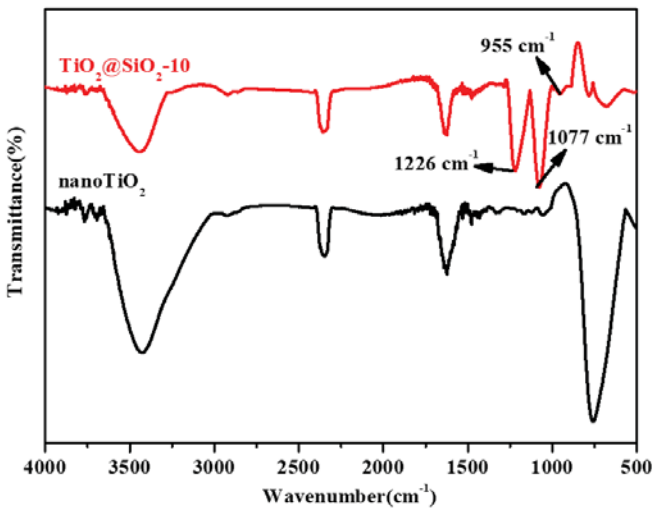

Figure 5: FT-IR spectra of nanoTiO$_2$ and TiO$_2$@SiO$_2$-10 sample.

955 cm^{-1}, assigned to asymmetric stretching of Si–O–Si linkages and Ti–O–Si bonds [31,32]. The appearance of these Si-related peaks provides direct spectroscopic evidence of successful silica coating. Vibrations in the 600–900 cm^{-1} region, present in both samples, are attributed to Ti–O bond stretching [8]. Significantly, after SiO_2 coating, the absorption band near 781 cm^{-1} shows a substantial decrease in intensity accompanied by a pronounced red shift of approximately 27 cm^{-1} compared to uncoated nano-TiO_2. This dual change—reduced intensity and frequency shift—is particularly diagnostic, as it results from lattice distortion and Ti–O–Si bond formation at the core-shell interface [13]. The magnitude of this shift (27 cm^{-1}) unambiguously confirms chemical bonding between the SiO_2 shell and TiO_2 core through partial substitution of Si for Ti, rather than mere physical adsorption. These complementary spectroscopic features collectively provide robust evidence for strong interfacial coupling in the TiO_2@SiO_2 structure.

The UV–vis transmittance spectra of TiO_2@SiO_2 samples synthesized at varying pH values were recorded to assess their ultraviolet shielding capabilities, with the results depicted in Figure 6. All samples demonstrated excellent transparency within the visible light range (400–800 nm), which can be attributed to the small size of TiO_2 nanoparticles (15–20 nm), less than half the wavelength of visible light, thereby allowing efficient passage of visible radiation. TiO_2 nanoparticles are commonly employed in sunscreen formulations, where maintaining visible-light transparency is essential for cosmetic acceptability. Conversely, a pronounced decrease in transmittance was observed in the UV region (200–400 nm) for the SiO_2-coated samples, corresponding to the strong absorption band of TiO_2 nanoparticles [31,32]. Notably, samples prepared under neutral to alkaline conditions exhibited UV transmittance values below 5%, indicative of substantial UV blocking ability [33,34]. This enhanced UV attenuation is likely due to the formation of a dense SiO_2 shell at these pH levels, which improves the ultraviolet light scattering efficiency of the TiO_2@SiO_2 composites.

The specific surface area and oil absorption capacity of TiO_2 are critical determinants of sunscreen tactile properties [35]. Figure 7 demonstrates how coating pH directly controls the Brunauer–Emmett–Teller (BET) surface area and oil absorption values of TiO_2@SiO_2 composites. Bare nano-TiO_2 exhibited the highest values—265.98 m^2/g BET surface area and 90.19 g/100 g oil absorption. Significantly, SiO_2 encapsulation dramatically reduced both parameters, with the reduction magnitude being strictly pH-dependent. Most notably, TiO_2@SiO_2-10 (synthesized at pH 10) achieved the lowest BET surface area and oil absorption among all samples, providing compelling evidence for the formation of a dense, minimally porous SiO_2 coating. This conclusion is strongly corroborated by electron microscopy observations, which independently confirmed the enhanced morphological compactness and density of the coating layer at this pH. Table 1 reveals critical differences in brightness (L) and Hunter Whiteness (Wh) values between bare nano-TiO_2 and SiO_2-coated TiO_2 samples prepared at various pH levels. Uncoated TiO_2 nanoparticles measured 96.86 for L and 92.02% for Wh. Significantly, SiO_2 encapsulation consistently enhanced these optical

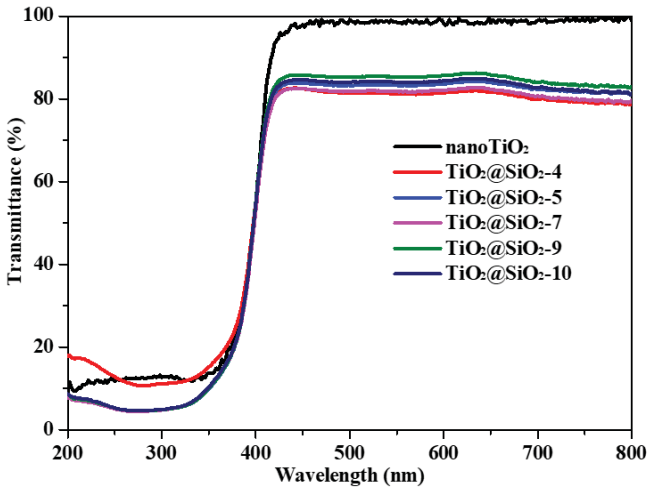

Figure 6: UV-vis transmittance spectra of nanoTiO$_2$ and TiO$_2$@SiO$_2$ samples.

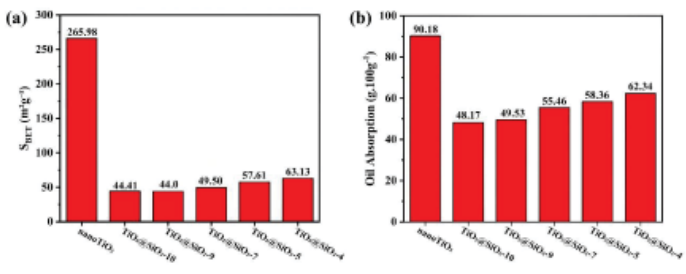

Figure 7: (a) S_{BET} and (b) oil absorption of nanoTiO$_2$ and TiO$_2$@SiO$_2$ samples.

Citation: Xiang W, Liu R, Liu J, Du C, Li L. Fabrication and Characterization of Cosmetic-grade TiO_2@SiO_2 for UV-shielding Ingredient. Int J Nanomater Nanotechnol Nanomed. 2026;12(1):0-11-017. Available from: https://dx.doi.org/10.17352/2455-3492.000074

properties, elevating brightness to 97.96 and whiteness to 94.03%. The coating pH exerted minimal influence on these parameters across the pH range tested. Most importantly, TiO_2@SiO_2-7 (synthesized at pH 7) achieved the highest brightness and whiteness values of all samples examined. This superior optical performance directly results from the enhanced dispersibility conferred by the SiO_2 coating, which demonstrably increases the brightness and whiteness of the coated powders by preventing particle agglomeration.

In order to make the TiO_2@SiO_2 sample useful in sunscreen, it is necessary to evaluate its fluidity, skin sensation, and sun protection factor (SPF). Table 2 presents the critical performance characteristics of sunscreens incorporating different TiO_2@SiO_2 samples. With TiO_2 content fixed at 15.6%, pH values remained consistent across all formulations. Crucially, the sunscreen containing TiO_2@SiO_2-10 exhibited markedly lower viscosity than the pristine nano-TiO_2 formulation—a direct consequence of the enhanced dispersibility imparted by the SiO_2 shell, which fundamentally improved fluidity by preventing TiO_2 aggregation. More significantly, SiO_2 coating dramatically elevated the SPF value from 29 to 41, representing a 41% enhancement in UV protection efficacy [36,37]. These compelling performance data unequivocally establish TiO_2@SiO_2-10 (synthesized at pH 10) as the superior formulation, demonstrating optimal properties that position it as the ideal candidate for ultraviolet filtration in commercial sunscreen products.

Conclusion

In this work, TiO_2@SiO_2 core-shell nanoparticles were fabricated successfully using a chemical deposition technique. The study focused on tuning the morphology of the SiO_2 coating by manipulating the reaction pH and SiO_2 content. Optimal coating was achieved at pH 10 with a SiO_2 loading of 10%, producing a uniform and continuous silica shell approximately 3 nm thick on TiO_2 surfaces. This configuration markedly improved the material's ultraviolet blocking capability. The TiO_2@SiO_2 sample prepared under these conditions demonstrated an impressive whiteness index of nearly 98% and an SPF value reaching 41. Such enhancements translate to better whitening effects, smoother skin feel, and increased compatibility for cosmetic formulations. Overall, this work introduces a straightforward and scalable method to produce densely coated TiO_2 particles, underscoring their promising applicability for industrial-scale cosmetic manufacturing.

Table 1: Color schemes of TiO_2@SiO_2 samples (in system CIE).

samples	L*	a*	b*	Hunter whiteness(Wh)/%
nanoTiO_2	96.86	-0.96	1.34	92.02
TiO_2@SiO_2-10	97.92	-0.58	1.13	93.96
TiO_2@SiO_2-9	97.90	-0.57	1.14	93.94
TiO_2@SiO_2-7	97.96	-0.59	1.13	94.03
TiO_2@SiO_2-5	97.87	-0.56	1.16	93.85
TiO_2@SiO_2-4	97.83	-0.59	1.19	93.70

Table 2: SPF of naked and TiO_2@SiO_2 samples (in system CIE).

Samples	Viscosity/mPa·s	pH	SPF	sensation
nanoTiO_2	7200	6.83	29	dry and loose
TiO_2@SiO_2-10	6300	6.91	41	Moisturizing

Acknowledgment

The authors gratefully acknowledge the support of the Scientific Research Foundation of Chongqing University of Technology (0115220003) and the Science and Technology Research Program of Chongqing Municipal Education Commission (Grant No. KJQN202201118).

(Supplementary-File)

References

1. Corinaldesi C, Marcellini F, Nepote E, Damiani E, Danovaro R. Impact of inorganic UV filters contained in sunscreen products on tropical stony corals (Acropora spp.). Sci Total Environ. 2018;637–638:1279–1285. Available from: https://doi.org/10.1016/j.scitotenv.2018.05.108

2. Zeng Y, He X, Ma Z, Gou Y, Wei Y, Pan S, et al. Coral-friendly and non-transdermal polymeric UV filter via the Biginelli reaction for in vivo UV protection. Cell Rep Phys Sci. 2023;4:101308. Available from: https://doi.org/10.1016/j.xcrp.2023.101308

3. Liu H, Zhang X, Ji B, Qiang Z, Karanfil T, Liu C. UV aging of microplastic polymers promotes their chemical transformation and byproduct formation upon chlorination. Sci Total Environ. 2023;858:159842. Available from: https://doi.org/10.1016/j.scitotenv.2022.159842

4. Singh A, Sheikh J. Preparation of mosquito repellent, antibacterial, and UV protective cotton using a novel, chitosan-based polymeric dye. Carbohydr Polym. 2022;290:119466. Available from: https://doi.org/10.1016/j.carbpol.2022.119466

5. Zhang J, Tian Z, Ji XX, Zhang F. Light-colored lignin extraction by ultrafiltration membrane fractionation for lignin nanoparticles preparation as UV-blocking sunscreen. Int J Biol Macromol. 2023;231:123244. Available from: https://doi.org/10.1016/j.ijbiomac.2023.123244

6. Zhang S, Wang T. Preparation of enzymolysis porous corn starch composite microcapsules embedding organic sunscreen agents and their UV protection performance and stability. Carbohydr Polym. 2023;314:120903. Available from: https://doi.org/10.1016/j.carbpol.2023.120903

7. Schneider LS, Lim HW. Review of environmental effects of oxybenzone and other sunscreen active ingredients. J Am Acad Dermatol. 2019;80(1):266–271. Available from: https://doi.org/10.1016/j.jaad.2018.06.033

8. Hamza EH, Shinya M, Takashi T, El-Hosainy H, Mine S, Toyao T, et al. Layered silicate stabilises diiron to mimic UV-shielding TiO2 nanoparticle. Mater Today Nano. 2022;19:100227. Available from: https://doi.org/10.1016/j.mtnano.2022.100227

9. Kim HJ, Roh DK, Chang JH, Kim DS. SiO2-coated platy TiO2 designed for noble UV/IR-shielding materials. Ceram Int. 2019;45:16880–16885. Available from: https://doi.org/10.1016/j.ceramint.2019.05.231

10. Lewicka ZA, Yu WW, Oliva BL, Contreras AQ, Colvin VL. Photochemical behavior of nanoscale TiO2 and ZnO sunscreen ingredients. J Photochem

Citation: Xiang W, Liu R, Liu J, Du C, Li L. Fabrication and Characterization of Cosmetic-grade TiO_2@SiO_2 for UV-shielding Ingredient. Int J Nanomater Nanotechnol Nanomed. 2026;12(1):0-11-017. Available from: https://dx.doi.org/10.17352/2455-3492.000074

Photobiol A. 2013;263:24–33. Available from: https://doi.org/10.1016/j.jphotochem.2013.04.019

11. Loosli F, Stoll S. Effect of surfactants, pH, and water hardness on the surface properties and agglomeration behavior of engineered TiO2 nanoparticles. Environ Sci Nano. 2017;4:203–211. Available from: https://doi.org/10.1039/C6EN00339G

12. Xie X, Liu YJ, Du WC, Hao JJ, Ma BL, Yang HW. Research of selective UV shielding material based on photonic crystals structure. Opt Mater. 2019;92:267–272. Available from: https://doi.org/10.1016/j.optmat.2019.04.044

13. Zhang YS, Yin HB, Wang AL, Ren M, Gu ZM, Liu YM, et al. Deposition and characterization of binary Al2O3/SiO2 coating layers on the surfaces of rutile TiO2 and the pigmentary properties. Appl Surf Sci. 2010;257(4):1351–1360. Available from: https://doi.org/10.1016/j.apsusc.2010.08.071

14. Sun J, Xu K, Shi C, Ma J, Li W, Shen X. Influence of core/shell TiO2@SiO2 nanoparticles on cement hydration. Constr Build Mater. 2017;156:114–122. Available from: https://doi.org/10.1016/j.conbuildmat.2017.08.124

15. Zhou J, Tan Z, Liu Z, Jing M, Liu W, Fu W. Preparation of transparent fluorocarbon/TiO2-SiO2 composite coating with improved self-cleaning performance and anti-aging property. Appl Surf Sci. 2017;396:161–168. Available from: https://doi.org/10.1016/j.apsusc.2016.11.014

16. Benz D, Bui HV, Hintzen HT, Kreutzer MT, van Ommen JR. Mechanistic insight into the improved photocatalytic degradation of dyes for an ultrathin coating of SiO2 on TiO2 (P25) nanoparticles. Chem Eng J Adv. 2022;10:100288. Available from: https://doi.org/10.1016/j.ceja.2022.100288

17. Pratima BM, Subrahmanyam A. Protective coatings on copper using as-deposited sol-gel TiO2-SiO2 films. Mater Today Proc. 2022;10:19. Available from: https://doi.org/10.1016/j.matpr.2022.11.463

18. Jaroenworaluck A, Pijarn N, Kosachan N, Stevens R. Nanocomposite TiO2–SiO2 gel for UV absorption. Chem Eng J. 2012;181–182:45–55. Available from: https://doi.org/10.1016/j.cej.2011.08.028

19. Guo J, Yuan S, Yu Y, van Ommen JR, Bui HV, Liang B. Room-temperature pulsed CVD-grown SiO2 protective layer on TiO2 particles for photocatalytic activity suppression. RSC Adv. 2017;7:4547–4554. Available from: https://doi.org/10.1039/C6RA27976G

20. Cho K, Chang H, Park JH, Kim BG, Jang HD. Effect of molar ratio of TiO2/SiO2 on the properties of particles synthesized by flame spray pyrolysis. J Ind Eng Chem. 2008;14(6):860–863. Available from: https://doi.org/10.1016/j.jiec.2008.06.010

21. Wang Y, Mo Z, Zhang C, Zhang P, Guo R, Gou H, et al. Morphology-controllable 3D flower-like TiO2 for UV shielding application. J Ind Eng Chem. 2015;32:172–177. Available from: https://doi.org/10.1016/j.jiec.2015.08.013

22. El-Toni AM, Yin S, Sato T, Ghannam T, Al-Hoshan M, Al-Salhi M. Investigation of photocatalytic activity and UV-shielding properties for silica-coated titania nanoparticles by solvothermal coating. J Alloys Compd. 2010;508:L1–L4. Available from: https://doi.org/10.1016/j.jallcom.2010.08.031

23. Asghar G, Dong X, Chae S, Saqlain S, Oh S, Choi KH, et al. Synthesis of TiO2 nanoparticle-embedded SiO2 microspheres for UV protection applications. Cryst Growth Des. 2023;23(2):256–262. Available from: https://doi.org/10.1021/acs.cgd.2c00983

24. Cheepborisutikui AJ, Ogawa M. Suppressing the photocatalytic activity of titania by precisely controlled silica coating. Inorg Chem. 2021;60(9):6201–6208. Available from: https://doi.org/10.1021/acs.inorgchem.0c03476

25. Chen Y, Liu R, Luo J. Improvement of anti-aging property of UV-curable coatings with silica-coated TiO2. Prog Org Coat. 2023;179:107479. Available from: https://doi.org/10.1016/j.porgcoat.2023.107479

26. Cao W, Wang A, Yin H. Preparation of TiO_2@ZrO_2@SiO_2@MAA nanocomposites and impact of layer structure on pigmentary performance. Mater Chem Phys. 2021;263:124403. Available from: https://doi.org/10.1016/j.matchemphys.2021.124403

27. Li L, Wang L, Chen XH, Tao CY, Du J, Liu ZH. The synthesis of bayberry-like mesoporous TiO2 microspheres by a kinetics-controlled method and their hydrophilic films. CrystEngComm. 2020;22:969–978. Available from: https://doi.org/10.1039/C9CE01824G

28. Li L, Chen XH, Xiong X, Wu XP, Xie ZN, Liu ZH. Synthesis of hollow TiO2@SiO2 spheres via a recycling template method for solar heat protection coating. Ceram Int. 2021;47:2678–2685. Available from: https://doi.org/10.1016/j.ceramint.2020.09.117

29. Chen PQ, Wei BZ, Zhu X, Gao DL, Gao YF, Cheng JG, et al. Fabrication and characterization of highly hydrophobic rutile TiO2-based coatings for self-cleaning. Ceram Int. 2019;45:6111–6118. Available from: https://doi.org/10.1016/j.ceramint.2018.12.085

30. Li L, Chen XH, Quan XJ, Qiu FC, Zhang XR. Synthesis of CuOx/TiO2 photocatalysts with enhanced photocatalytic performance. ACS Omega. 2023;8:2723–2732. Available from: https://doi.org/10.1021/acsomega.2c07364

31. Bai Y, Li Z, Cheng B, Zhang M, Su K. Higher UV-shielding ability and lower photocatalytic activity of TiO2@SiO2/APTES and its excellent performance in enhancing the photostability of poly(p-phenylene sulfide). RSC Adv. 2017;7:21758. Available from: https://doi.org/10.1039/c6ra28098f

32. Altinisik S, Kortun A, Nazh A, Cengiz U, Koyuncu S. PEG-functionalized carbazole-based polymers for UV-protected hydrophilic glass coatings. Prog Org Coat. 2023;175:107352. Available from: https://doi.org/10.1016/j.porgcoat.2022.107352

33. Zhang Y, Wu YF, Chen M, Wu LM. Fabrication method of TiO2–SiO2 hybrid capsules and their UV-protective property. Colloids Surf A. 2010;353:216–225. Available from: https://doi.org/10.1016/j.colsurfa.2009.11.016

34. Dalanta F, Kusworo TD, Aryanti N. Synthesis, characterization, and performance evaluation of UV light-driven Co-TiO2@SiO2 based photocatalytic nanohybrid polysulfone membrane for effective treatment of petroleum refinery wastewater. Appl Catal B Environ. 2022;316:122576. Available from: https://doi.org/10.1016/j.apcatb.2022.121576

35. Guo QR, Wei DB, Zhao CF, Wang CP, Ma HJ, Du YG. Physical UV-blocker TiO2 nanocomposites elevated toxicity of chemical sunscreen BP-1 under UV irradiation. Chem Eng J. 2023;469(1):143899. Available from: https://doi.org/10.1016/j.cej.2023.143899

36. Swain B, Park JR, Park KS, Lee CG. Synthesis of cosmetic grade TiO2-SiO2 core-shell powder from mechanically milled TiO2 nanopowder for commercial mass production. Mater Sci Eng C Mater. 2019;95:95–103. Available from: https://doi.org/10.1016/j.msec.2018.10.005

37. Masanori H, Sakiko S, Haruhisa K, Yosuke T, Ayako N, Yasukazu Y. Does the photocatalytic activity of TiO2 nanoparticles correspond to photo-cytotoxicity? Cellular uptake of TiO2 nanoparticles is important in their photo-cytotoxicity. Toxicol Mech Methods. 2016;26(4):284–294. Available from: https://doi.org/10.1080/15376516.2016.1175530

Citation: Xiang W, Liu R, Liu J, Du C, Li L. Fabrication and Characterization of Cosmetic-grade TiO_2@SiO_2 for UV-shielding Ingredient. Int J Nanomater Nanotechnol Nanomed. 2026;12(1):0-11-017. Available from: https://dx.doi.org/10.17352/2455-3492.000074